RXRα Deficiency Confers Genetic Susceptibility for Aortic Sac, Conotruncal, Atrioventricular Cushion, and Ventricular Muscle Defects in Mice

Peter J. Gruber,* Steven W. Kubalak,* Tomas Pexieder,‡† Henry M. Sucov,§ Ronald M. Evans,‖ and Kenneth R. Chien*

*Department of Medicine, Center for Molecular Genetics, and the American Heart Association-Bugher Foundation Center for Molecular Biology, University of California, San Diego, La Jolla, California 92093-0613; ‡Institute d'Histologie et d'Embryologie, Université de Lausanne, 1005 Lausanne, Switzerland; §University of Southern California, School of Medicine, Department of Cell and Neurobiology, Institute for Genetic Medicine, Los Angeles, California 90033; and ‖Gene Expression Laboratory, Howard Hughes Medical Institute, The Salk Institute for Biological Studies, La Jolla, California 92138

Abstract

Retinoid-dependent pathways play a central role in regulating cardiac morphogenesis. Recently, we characterized gene-targeted *RXRα* −/− embryos, which display an atrial-like ventricular phenotype with the development of heart failure and lethality at embryonic day 14.5. To quantitate the frequency and complexity of cardiac morphogenic defects, we now use microdissection and scanning electron microscopy to examine 107 wild-type, heterozygous, and homozygous embryos at embryonic day 13.5, 14.5, and 15.5. *RXRα* −/− embryos display complex defects, including ventricular septal, atrioventricular cushion, and conotruncal ridge defects, with double outlet right ventricle, aorticopulmonary window, and persistent truncus arteriosus. In addition, heterozygous *RXRα* embryos display a predisposition for trabecular and papillary muscle defects, ventricular septal defects, conotruncal ridge defects, atrioventricular cushion defects, and pulmonic stenosis. Lastly, we show that the intermediate anatomic phenotype displayed by heterozygous embryos is mirrored in the molecular marker *MLC-2a*. The intermediate phenotype of *RXRα* heterozygous embryos documents a gene dosage effect for *RXRα* in maintaining normal cardiac morphogenesis. In addition, some defects in *RXRα* mutant mice are phenocopies of human congenital heart defects, thereby suggesting that a relative deficiency in *RXRα* or molecules downstream in its signaling pathway may represent congenital heart disease–susceptibility genes. (*J. Clin. Invest.* 1996. 98:1332–1343.) Key words: mouse • congenital • development • heart • vitamin A

Introduction

Congenital heart disease affects 1 in 200 live births in the United States with a wide range of distinct phenotypes for which there are few recognized candidate genes or even broad molecular insights (1). The identification of the genetic determinants of complex congenital heart disease has been con-founded by its sporadic nature, incomplete penetrance with variable clinical phenotypes, and presumptive polygenic, multifactorial etiology. One approach to identifying genetic determinants of congenital heart disease has been to examine monogenic disorders that are associated with congenital malformations. This type of approach has been successful for supravalvular aortic stenosis, where the defect is apparently based upon a deficiency in the elastin gene product (2). A number of other genetic disorders are associated with cardiovascular developmental defects, such as Holt-Oram syndrome, Down's syndrome, and the microdeletions on chromosome 22 associated with DiGeorge syndrome (3–7). However, the precise identity of the gene products in these syndromes is currently unknown.

An alternative approach to identifying genes that may be responsible for congenital heart disease is to examine the role of candidate genes with murine gene–targeted models of cardiogenesis. In this regard, recent studies have provided direct evidence that retinoid signaling may be critical for the maintenance of normal cardiac morphogenesis. Heart defects have also been observed in animals fostered under conditions of vitamin A deficiency, leading to defects in ventricular chamber morphogenesis as well as multiple noncardiac effects (8–10). Signals derived from vitamin A and its metabolites alter patterns of gene expression through the action of retinoid receptors, members of the steroid hormone receptor superfamily of ligand-dependent transcription factors. These receptors comprise two distinct subfamilies composed of three retinoic acid receptors (RARα, β, γ)[1] and three retinoic X receptors (RXRα, β, γ). These two groups share overlapping ligand specificity since both receptors bind 9-*cis* retinoic acid with high affinity, while only the RARs bind all-*trans* retinoic acid. It has been shown in vitro that RXRs are able to bind DNA as homodimers, whereas RARs as well as receptors for thyroid hormone, vitamin D, and peroxisome proliferators form heterodimers with *RXRs* that bind DNA in a highly cooperative fashion. Recently, the role of these receptors in cardiovascular development has been explored through systematic gene targeting of each member of the retinoid receptor family. While mice with knockouts of the *RARα* (11, 12), *RARβ* (13), or *RARγ* (14) genes display no obvious cardiovascular defects, mice that contain double knockouts of *RAR* isoforms display abnormalities of the aortic arches and outflow tract (15). In ad-

1. *Abbreviations used in this paper:* DORV, double outlet right ventricle; ed, embryonic day; EF1α, elongation factor 1α; MLC-2a, atrial myosin light chain; PTA, persistent truncus arteriosus; RAR, retinoic acid receptor; RT, room temperature; RXR, retinoic X receptor; SEM, scanning electron microscopy; VSD, ventricular septal defect.

dition, recent studies have documented that a single gene knockout of the *RXRα* gene results in severe cardiac muscle defects associated with a deficiency in expansion of the compact zone and a consequent decrease in cardiac function (16, 17). The decrease in cardiac muscle mass results in embryonic heart failure and lethality around embryonic day (ed) 14.5 as assessed by miniaturized physiological technology in the living embryo (18). This defect is similar to a subset of the cardiovascular alterations seen in the setting of vitamin A deficiency, suggesting that *RXRα*-dependent pathways are critical in the maintenance of normal cardiac morphogenesis.

The question arises whether *RXRα* deficiency would produce an increased frequency of other complex cardiac morphogenic defects that would lie in other tissue compartments of the heart including the aortic sac, conotruncal ridges, atrioventricular cushions, or subtle defects of ventricular morphogenesis. This type of study necessitates a rapid, quantitative approach to score for all of the potentially complex malformations that could occur in each of these compartments during various stages of murine cardiac morphogenesis. By examining relatively large numbers of wild-type, heterozygous, and homozygous embryos, one can quantitatively score for the appearance of relatively infrequent yet severe cardiovascular malformations that may arise as a result of variable levels of *RXRα* deficiency. Additionally, one can determine whether any of these resulting phenotypes resemble known cardiovascular malformations in man. Using a rapid throughput microdissection protocol in combination with scanning electron microscopy (19), we now report the detailed analysis of cardiac morphogenic defects in *RXRα*-deficient embryos. Interestingly, mice that are heterozygous for *RXRα* also display a number of cardiac abnormalities, with defects in both cushion mesenchyme, manifest as pulmonic stenosis and atrioventricular cushion defects, and muscle, manifest as right or left ventricular hypoplasia and trabecular disarray. Additionally, we identify a molecular marker *MLC-2a* whose expression mirrors the anatomic analysis in that its expression level is intermediate between wild-type and homozygous embryos.

These studies indicate that there is a critical requirement for *RXRα*, not only in the muscle compartment, but also in the formation of the endocardial cushions of both the atrioventricular region and the conotruncus. Thus, a knockout of a single member of the retinoid receptor gene family can result in multiple defects to virtually every compartment of the developing heart, implying a central role for *RXRα* in cardiac morphogenesis. To our knowledge, no other single gene-targeted event of any of the other retinoid receptors has thus far been associated with cardiovascular defects. This underscores a particularly important role for *RXRα* in orchestrating and maintaining normal cardiac morphogenesis. In addition, finding cardiac defects in heterozygous embryos resembling forms of human congenital malformations, such as pulmonic stenosis, cleft mitral valve, and selective chamber dysplasia, implicates *RXRα* as a possible candidate for conferring genetic susceptibility for congenital heart disease phenotypes, and provides evidence for a threshold effect for *RXRα* for activating specific steps of cardiac morphogenesis.

Methods

Breeding and identification of gene-targeted mice. RXRα −/− mutant mice in a C57/Bl6 background were maintained in colonies and bred

as described (16). The genotype of individual animals was determined by PCR analysis of tail or hind limb DNA extracts. Briefly, tissue samples were digested overnight in tail extraction buffer (10 mM Tris-HCl, 100 mM NaCl, 10 mM EDTA, 0.5% SDS, pH 8.0) with 80 μg/ml proteinase K. DNA was precipitated with an equal volume of isopropanol and resuspended in 10 mM Tris-HCl, 1 mM EDTA, pH 8.0. Oligonucleotide primers were designed to give a 600-bp band by agarose gel electrophoresis for the wild-type allele and a 400-bp band for the targeted allele.

Microdissection and scanning electron microscopy. Using pipettes with sharply beveled tips (20), hearts of harvested embryos were fixed in end-diastole by intraventricular high flow–low pressure perfusion fixation (21) with 2% glutaraldehyde, 1% formaldehyde in 1% cacodylate buffer made isotonic with NaCl. Perfusion was followed by immersion in the same fixative for storage. A standardized procedure for microdissection and scanning electron microscopy (SEM) analysis of the heart was applied (19). Using an operating microscope (Wild M690; Leica, Heerbrugg, Switzerland), the hearts were exposed and examined. In the case of abnormal morphology, macrophotographs of the frontal aspect as well as of the left and right profiles were taken with a photomicroscope (Wild Photomacroscope M400; Leica, Heerbrugg, Switzerland). In all specimens, the right ventricle was cut with crafted microscissors proceeding from the apex into the pulmonary artery trunk and the ductus arteriosus. Similarly, the left ventricle was cut open from the apex towards the base of the heart and its internal relief examined. The ventricular cavity and the conotruncus were scrutinized for anomalies and photographed. Subsequently, the parietal and septal segments of the right ventricle as well as the parietal segment of the left ventricle were isolated by extending the previously mentioned cuts of the right and left ventricles beyond the base of the heart. These segments were submitted to ethanol dehydration and critical point drying from Freon 113 to Freon 23 (CPD 030 apparatus; Balzers S.p.A., Milan, Italy). Dried specimens were mounted on SEM tubes, ion sputtered (S150; Edwards Co., Santa Ana, CA) with 300 nm gold, and examined in the scanning electron microscope (JSM 6300-F; JEOL U.S.A. Inc., Peabody, MA). SEM photomicrographs were taken in standard orientations and magnifications. Primary magnification of all photomacrographs was 20×. Primary magnification of scanning electron micrographs was 60×. The genotype and phenotype analyses were performed under double-blind conditions.

Linear measurements of right and left ventricular compact zone thickness were made on prints of SEM photomicrographs using calipers immediately inferior to the tricuspid and mitral orifices, respectively. The precision of the measurements was 0.24 μm. A generalized linear model for analysis of variance using Chi squared and Fischer's exact test was performed with right and left ventricular compact zone thickness as dependent variables and age, genotype, and the presence, absence, or type of anomaly as sources of variation.

Whole heart in situ hybridization. Whole heart in situ hybridization was performed using modifications of the procedure described by Wilkinson (22). An atrial myosin light chain (MLC-2a) riboprobe template was produced by AvaII restriction of a plasmid containing the *MLC-2a* gene (AMLC210). A digoxigenin-labeled cRNA probe was generated using T7 polymerase and the 10× DIG RNA labeling mixture obtained from Boerhinger Mannheim Biochemicals (Indianapolis, IN) and used per the manufacturer's recommendations.

Embryonic hearts were dissected free from surrounding tissues and further dissected to remove the apices of the right and left ventricles and the right and left atria (thus reducing trapping of the color precipitate). The specimens were fixed overnight at 4°C in 4% paraformaldehyde/PBS before sequential 5-min washes at room temperature (RT) in PBS, PBS, 25, 50, 75, 100, 100, 75, 50, and 25% methanol, and PBT (PBS, 0.1% Tween-20) twice. Embryos were bleached for 1 h at RT with 6% hydrogen peroxide/PBS followed by three PBT washes. Digestion for 10 min at 37°C with 15 μg/ml proteinase VIII was followed by 5-min washes in 2 mg/ml glycine/PBS, and three times in PBT. Embryos were prehybridized at 70°C for at least 6 h with hybridization buffer (50% deionized formamide/5×

SSC, pH 4.5, 50 μg/ml yeast RNA, 50 μg/ml heparin, 1% SDS) before replacing the solution along with the addition of riboprobe at 1 μg/ml; hybridization took place for 20–36 h at 70°C. Sequential 15-min washes were performed with solution 1 (5× SSC, pH 4.5, 50% formamide, 1% SDS) at 70°C three times, 1:1 mix of solution 1 and solution 2 (0.5 M NaCl, 10 mM Tris-HCl, pH 7.5, 0.1% Tween-20) at 70°C twice, and solution 2 three times at RT. RNase digestion was performed in solution 2 at 37°C with 75 μg/ml RNase A and 75 μg/ml RNase T1 twice for 30 min. Sequential 15-min washes were then performed at RT with solution 2, and twice with solution 3 (50% formamide, 2× SSC, pH 4.5) before a 30-min wash at 65°C with solution 3. Embryos were then rinsed three times at RT in TBST (0.8 g NaCl, 0.02 g KCl, 2.5 ml 1 M Tris-HCl, pH 7.5, 1.0 ml 10% Tween-20, 4 mM Levamisole) and then blocked for 1 h at RT with 10% normal sheep serum (NSS)/TBST. Alkaline phosphatase–conjugated antidigoxigenin sheep Fab fragments (Boerhinger Mannheim Biochemicals) were used to detect the hybridized transcripts; this was diluted at 1:2,000 in 2% NSS/TBST and incubated with the embryos at 4°C for 16–24 h.

Sequential, 1-h, postantibody washes were performed at RT five times with TBST, followed by five 10-min washes at RT with NTMT (100 mM NaCl, 100 mM Tris-HCl, pH 9.5, 25 mM MgCl₂, 0.1% Tween-20, 4 mM Levamisole). The color reaction was performed at RT with 4.5 μl 75 mM nitro blue tetrazolium (Boerhinger Mannheim Biochemicals) and 3.5 μl 75 mM X-phosphate (Boerhinger Mannheim Biochemicals) until an intense blue color appeared. The reaction was stopped in 10 mM Tris, pH 7.4, 1 mM EDTA, pH 8.0, and embryos postfixed for 2 h at RT in 4% paraformaldehyde/PBS.

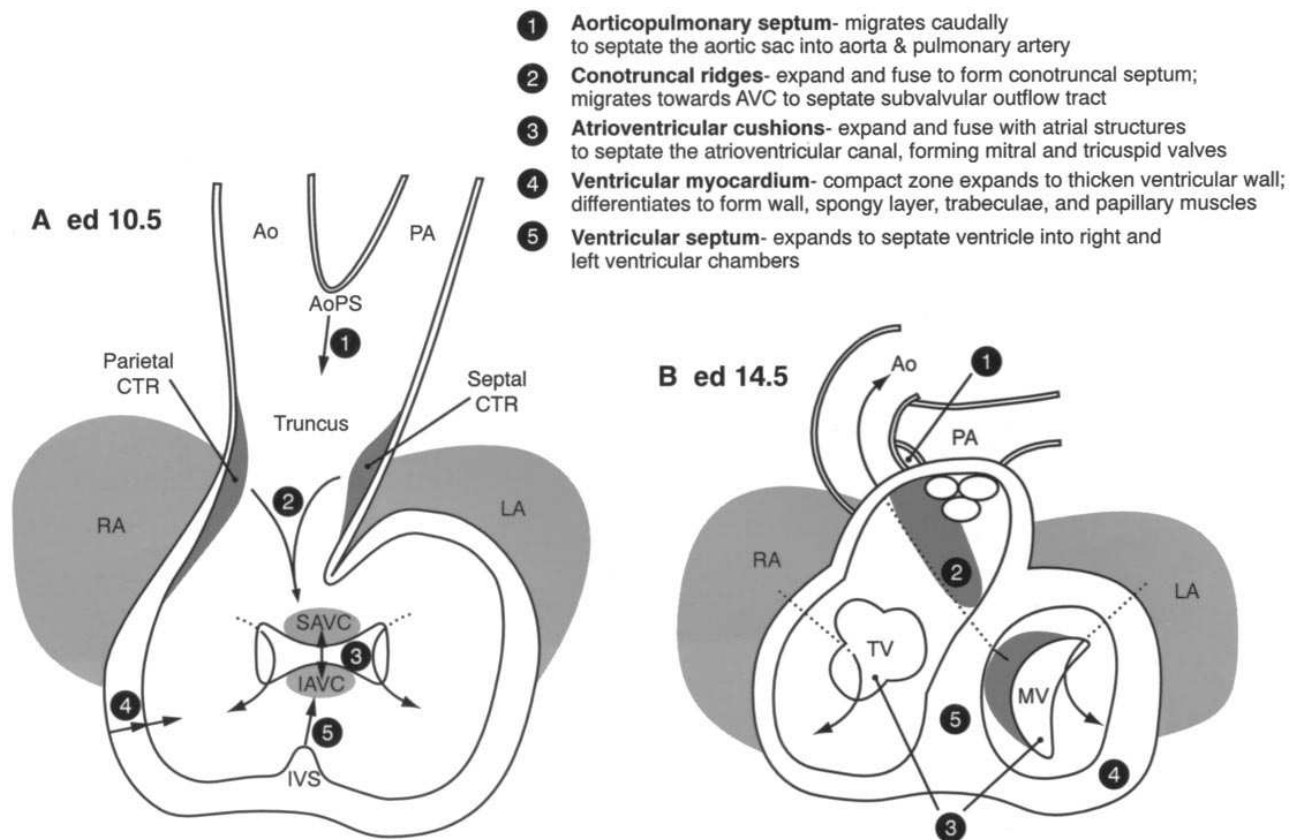Specimens were photographed with a stereomicroscope (SV6; Carl Zeiss, Inc., Thornwood, NY) and slides digitized. Figures were composed in Adobe Photoshop 3.0, QuarkXPress 3.31, and printed by Fujix Pictography (Fuji Photo Film Co., Tokyo, Japan).

Ribonuclease protection assays. RNase protection assays were performed per the manufacturer's recommendations using the Direct Protect Lysate Ribonuclease Protection Assay kit from Ambion, Inc. (Austin, TX). Left ventricular free wall samples were dissected from individual day 13.5 embryonic hearts and placed in 50 μl of lysis solution at room temperature for 5 min. Samples were then vortexed to lyse the tissue and stored at −20°C. For the assessment of the expression of the mouse *MLC-2a* gene, a 355-bp probe (285-bp protected fragment using T7 polymerase) was generated by AvaII restriction of a plasmid containing the *MLC-2a* gene (AMLC210). For the assessment of the expression of the mouse ventricular myosin light chain gene, a 230-bp probe (169-bp protected fragment using T7 polymerase) was generated by Sau3AI restriction of a plasmid containing the *MLC-2v* gene (MLC510). The expression of elongation factor 1α (EF1α) was used as a loading control and a 140-bp probe (100-bp protected fragment using SP6 polymerase) was generated by DdeI restriction of a plasmid containing the EF1α. Riboprobes were generated using the MAXIscript In Vitro Transcription kit from Ambion, Inc. per the manufacturer's recommendations. 1 μg of template was used in each synthesis reaction with fragments labeled by [³²P]CTP and purified on an 8 M urea, 6% polyacrylamide gel. Samples in lysis solution were hybridized with 100,000 cpm of the purified probe at 37°C overnight. The unprotected RNA was subsequently digested with RNases A and T1 at 37°C for 30 min. The reaction was terminated with sarcosyl and proteinase K, and the reaction mixture precipitated with 0.6 vol 100% isopropanol. The RNase-resistant hybrids were analyzed by gel electrophoresis on a denaturing polyacrylamide/urea gel. The gel was dried and autoradiography performed until a signal was detected.

Table I. Heart Defects in RXRα Gene-targeted Embryos

Tissue compartment	Phenotype	Frequency of defects (%)		
		−/− (18)*	+/− (60)	+/+ (29)
Aortic sac (7)‡	Absent aorticopulmonary septum/ persistent truncus arteriosus	11 (2)	0 (0)	0 (0)
	Incomplete aorticopulmonary septum/ aorticopulmonary window	28 (5)	0 (0)	0 (0)
	Pulmonary artery stenosis§	0 (0)	2 (1)	0 (0)
Conotruncus (38)	Absent conotruncal ridges	66 (6)	3 (2)	0 (0)
	Hypoplastic conotruncal ridges§	6 (1)	0 (0)	0 (0)
	Hyperplastic conotruncal ridges	0 (0)	2 (1)	0 (0)
	Short conotruncal septum	28 (5)	7 (4)	0 (0)
	Double outlet right ventricle	17 (3)	5 (3)	0 (0)
Atrioventricular canal (42)	Hypoplastic cushions	67 (12)	8 (5)	0 (0)
	Absent fusion	39 (7)	3 (2)	0 (0)
	Incomplete fusion	33 (6)	11 (7)	0 (0)
	Cleft mitral valve‖	17 (3)	17 (11)	23 (7)
	Cleft tricuspid valve	17 (3)	8 (5)	0 (0)
Myocardium (78)	Hypoplastic compact zone	94 (17)	5 (3)	0 (0)
	Ventricular septal defect	94 (17)	52 (31)	0 (0)
	Disorganized trabeculae	67 (12)	49 (32)	13 (4)
	Dysplastic papillary muscles			
	right ventricular	39 (7)	54 (35)	0 (0)
	left ventricular	17 (3)	32 (21)	0 (0)
	Papyraceous ventricles§			
	right	0 (0)	2 (1)	0 (0)
	left	0 (0)	2 (1)	0 (0)

*Numbers in parentheses refer to the total number of embryos harboring a defect for each genotype. ‡Numbers in parentheses in the first column refer to the total number of embryos harboring a defect in the designated tissue compartment. §P > 0.05. All other frequencies are significantly different to P < 0.001. ‖Clefts seen in −/− and +/− embryos have a different morphology from that seen in +/+ embryos.

1. **Aorticopulmonary septum**- migrates caudally to septate the aortic sac into aorta & pulmonary artery

2. **Conotruncal ridges**- expand and fuse to form conotruncal septum; migrates towards AVC to septate subvalvular outflow tract

3. **Atrioventricular cushions**- expand and fuse with atrial structures to septate the atrioventricular canal, forming mitral and tricuspid valves

4. **Ventricular myocardium**- compact zone expands to thicken ventricular wall; differentiates to form wall, spongy layer, trabeculae, and papillary muscles

5. **Ventricular septum**- expands to septate ventricle into right and left ventricular chambers

Figure 1. Critical structures in cardiac development. Four distinct tissue compartments of the heart develop via distinct mechanisms. (*1*) The aorticopulmonary septum exists as a migrating mass of neural crest–derived cells. The distal boundary of its migration lies somewhat below the level of the semilunar valves. (*2*) The conotruncal cushions begin as a pair of spiral mesenchymal swellings in the primordial ventricular outflow tract, eventually fusing to form the conotruncal septum. This divides the subvalvular outflow tract and contributes to the membranous interventricular septum. (*3*) The atrioventricular cushions, like the conotruncal cushions, begin as a pair of mesenchymal swellings in the atrioventricular canal, which connects the common atrium with the common ventricle. The fusion of these cushions along with the contribution of atrial structures (not shown) contribute to the septation of the common atrioventricular canal into the right (tricuspid) and left (mitral) atrioventricular orifices. (*4* and *5*) The myocardium begins as a single layer of cells beneath the epicardium. These proliferate and differentiate into the expanded compact zone and specialized myocardial tissue trabeculae from which papillary muscles form. *Ao*, aorta; *PA*, pulmonary artery; *LA*, left atrium; *TV*, tricuspid valve; *MV*, mitral valve; *AoPS*, aorticopulmonary septum; *CTR*, conotruncal ridge; *SAVC*, superior atrioventricular cushion; *IAVC*, inferior atrioventricular cushion; *IVS*, interventricular septum.

Results

Aorticopulmonary septum and cushion tissue mesenchyme defects in RXRα −/− embryos. Examination of 18 *RXRα* homozygous null embryos by microdissection and SEM revealed multiple phenotypes in four distinct compartments of the heart: aortic sac (that area of the ventricular outflow tract above the semilunar valves), conotruncus (that area of the ventricular outflow tract below the semilunar valves), atrioventricular cushions (mesenchymal tissue dividing the atrial and ventricular chambers), and ventricular myocardium. Table I lists the defects found in each of the distinct tissue types for each *RXRα* genotype.

Defects in normal septation of the aortic sac are related to abnormalities in formation of the aorticopulmonary septum. Figs. 1 and 2 schematically diagram the normal maturation of each tissue compartment. Fig. 1, *A* is a representation of an ed 10.5 mouse embryonic heart in which complete septation of the aortic sac has not yet occurred. Fig. 1, *B* diagrams an ed

14.5 mouse embryonic heart in which migration of the aorticopulmonary septum has completely divided the supravalvular ventricular outflow tract into the aorta and main pulmonary artery. Fig. 3 shows examples of the major findings with the first column demonstrating normal specimens, the second column defects of intermediate severity, and the third column the most severe defects. Incomplete formation or migration of aorticopulmonary septum tissue results in either aorticopulmonary window in the partial case or persistent truncus arteriosus (PTA) in the complete case. Though relatively infrequent, *RXRα* homozygous embryos demonstrated both aorticopulmonary window (28%, Fig. 3 *b*) and PTA (11%, Fig. 3 *c*). Compared to wild type embryos (Fig. 3 *a*), the extent of aorticopulmonry septum migration as indicated by the solid arrow is reduced. Defects in the aortic sac are the least frequent abnormalities seen as only seven embryos displayed abnormalities in this tissue compartment.

The subvalvular ventricular outflow tract septates in a complex series of events that begin as the formation of cushion

structures derived through interactions between the myocardium and endocardium. The parietal and septal conotruncal ridges form in a spiral fashion (Fig. 1 *A*) and eventually fuse to create a structure called the conotruncal septum, normally dividing the conotruncus into the right (pulmonary artery) and left (aorta) ventricular outflow tracts (Figs. 1 *B* and 3 *d*) by ed 12.5. 100% of *RXRα* homozygous null mutants have abnormalities of conotruncal ridges ranging from mild deficiency of conotruncal tissue (6%, Fig. 3 *e*, indicated by the short double-headed arrow) to complete absence of cushion tissue (66%, Fig. 3 *f*, normal position indicated by a dotted, double headed arrow). A portion of embryos with shortened conotruncal ridges precisely mimicked the human condition of ventricular septal defect (VSD)–type double outlet right ventricle (DORV) (17%, Fig. 3 *e*). Deficiencies of the aorticopulmonary septum and conotruncus were not coincident, suggesting that mutually exclusive mechanisms may be responsible for their formation.

The atrioventricular cushions, along with atrial structures, are responsible for dividing the atrioventricular canal into right (tricuspid) and left (mitral) orifices. They arise, as do the conotruncal ridges, from interactions between the muscle and endocardium resulting in transformation into mesenchymal cushions (Fig. 1 *A*) and definitively into mature valvular structures (Figs. 1 *B* and 2 *A*). However, incomplete formation or fusion of the atrioventricular cushions can result in defects ranging from small clefts in valve leaflets (Fig. 2 *B*) to complete lack of atrioventricular septation and atrioventricular canal (Fig. 2 *C*). *RXRα* homozygous embryos exhibit the entire spectrum of severities. Deficiencies of the atrioventricular cushions range from cleft mitral valve (17%, Fig. 3 *f*) and cleft tricuspid valve (17%) to common atrioventricular canal and complete lack of fusion of the superior and inferior atrioventricular cushions (39%, Fig. 3, *h* and *i*). Intermediate were 12 embryos (67%) with partial fusion of the atrioventricular cush-

ions. However, even in those animals in which a common atrioventricular canal was seen, primordial cushion tissue was always observed (Fig. 3 *i*), suggesting that the defect is a result of cushion growth, maturation, or fusion deficiency rather than interference with their initial induction. This is in marked contrast to the conotruncus, in which all cushion tissue was occasionally absent (Fig. 3 *f*).

Myocardial architecture defects in RXRα −/− embryos. The myocardium expands from a thin layer of cells beneath the epicardium to form a thicker compact zone of muscle (Fig. 1, *A* and *B*). Additionally, some myocytes form specialized structures called trabeculae that project across portions of the ventricular cavity. The transition zone between these two tissues is called the spongy layer. In *RXRα* homozygous embryos, the ventricular myocardium was the most frequently and severely affected tissue type. It has been noted previously (16, 17), resulting in a hypoplastic compact zone (94%, Fig. 4 *b*) and isolated ventricular septal defect (94%, Fig. 4 *c*). However, ventricular septal defects were not only confined to the membranous septum (a structure largely derived from the fusion of three tissues—conotruncal septum, atrioventricular cushion, and ventricular septum), but sometimes also included the muscular portion, resulting in large interventricular defects. All defects listed in Table I as ventricular septal defects were muscular. Additionally, defects in the spongy and trabeculated layers of the myocardium occurred frequently. The spongy layer of the myocardium was generally thicker in mutant embryos (Fig. 4 *b*) than in wild-type embryos (Fig. 4 *a*). Trabeculae were attenuated (67%, Fig. 4 *f*) and contained an unusual, random branching pattern as compared with the more parallel branching pattern found in normal embryos. Papillary muscles joining atrioventricular valvular leaflets to the ventricular wall likely develop as specialized trabeculae. Not surprisingly, dysmorphic papillary muscles were often observed (56%, Fig. 4 *e*).
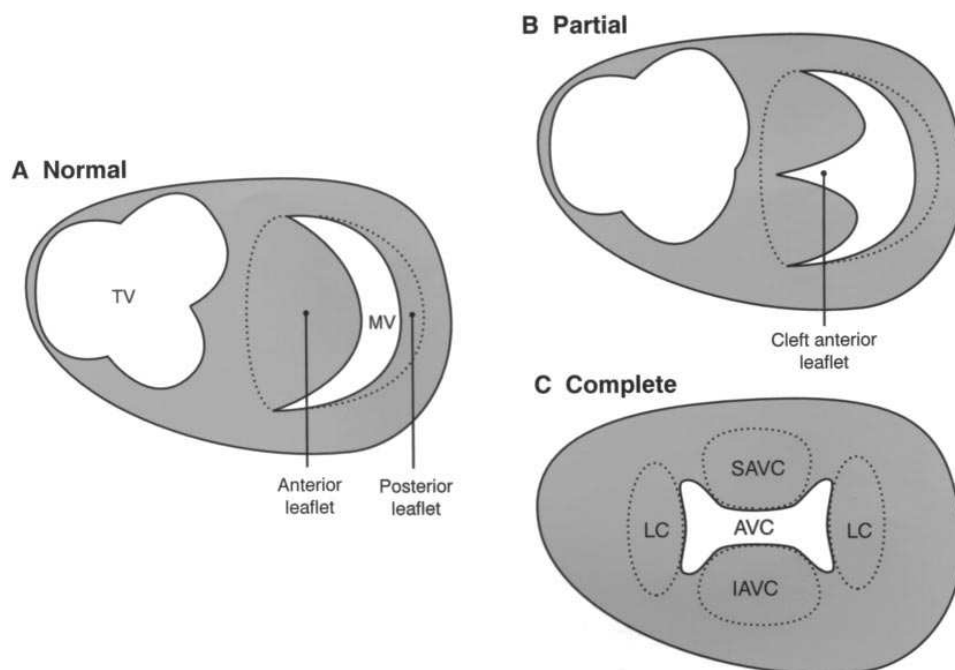

Figure 2. Atrioventricular cushion development. (*A*) Complete fusion of the atrioventricular cushions along with atrial structures (not shown), results in formation of the mitral and tricuspid orifices. (*B*) Incomplete fusion of the SAVC and IAVC results in a residual cleft in the anterior mitral leaflet. (*C*) A common canal connects the atria with the ventricles. *TV*, tricuspid valve; *MV*, mitral valve; *SAVC*, superior atrioventricular cushion; *IAVC*, inferior atrioventricular cushion; *LC*, lateral cushions.
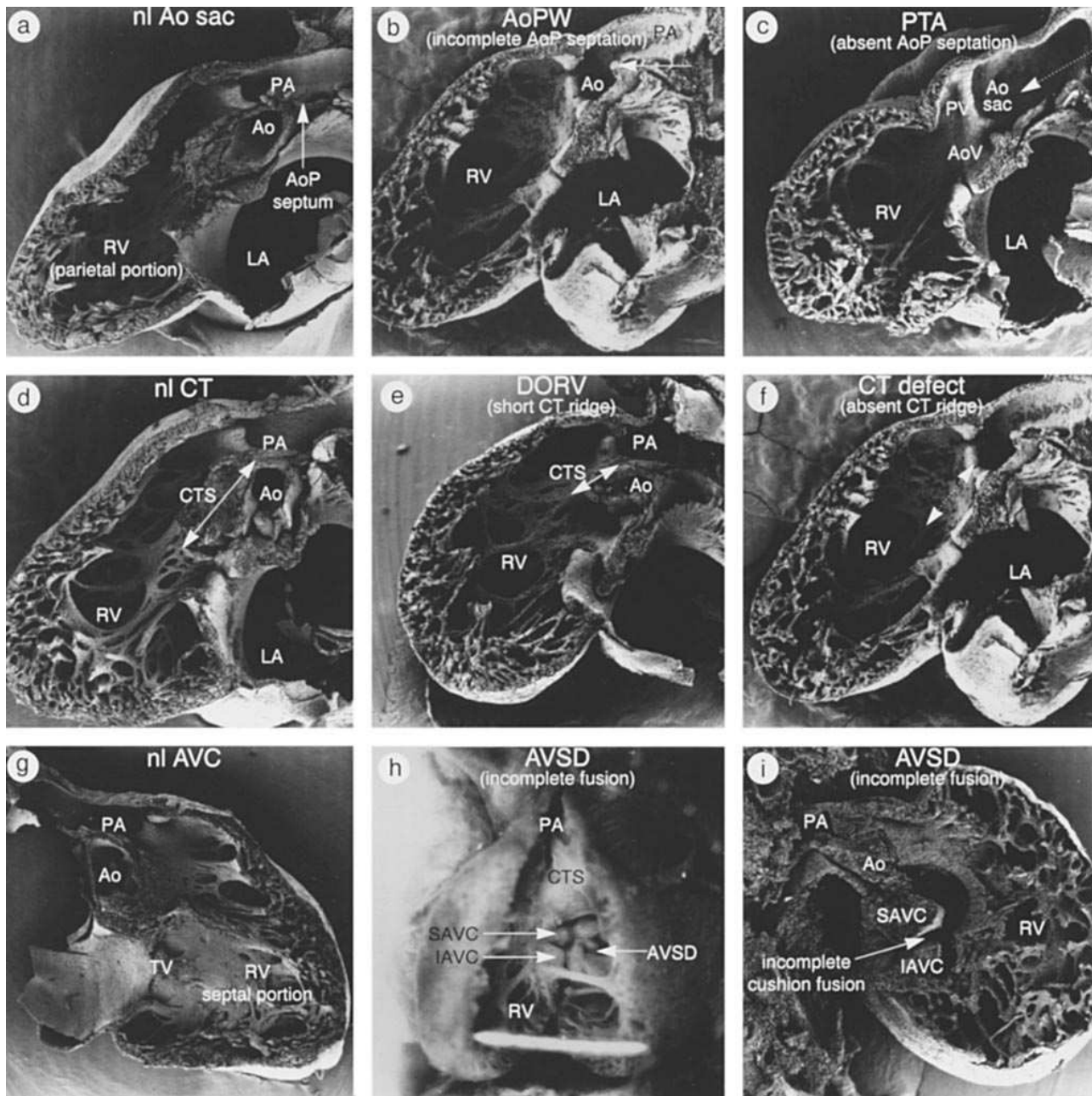
Figure 3. Cushion mesenchyme defects in *RXRα −/−* embryos. Light macrophotograph (*h*) and SEM (*a–g*, and *i*) of perfusion-fixed, microdissected *RXRα −/−* mouse embryos demonstrating aortic sac defects (aorticopulmonary window [*b*] and persistent truncus arteriosus [*c*]), conotruncal defects (double outlet right ventricle [*e*] and aplastic conotruncal ridges [*f*]), and atrioventricular cushion defects (atrioventricular septal defects [*h*] and hypoplastic atrioventricular cushions [*i*]). The first column shows examples of normal aortic sac (*a*), conotruncus (*d*), and atrioventricular cushion (*g*); the second and third columns demonstrate defects in each of the tissue types in order of increasing severity. In the second row (*d–f*), double-headed arrows demonstrate the extent of the conotruncal septum with the dotted line in *f* indicating the proper location of the absent conotruncal cushion tissue. *Ao*, aorta; *PA*, pulmonary artery; *AoV*, aortic valve; *PV*, pulmonic valve; *RV*, right ventricle; *LV*, left ventricle; *LA*, left atrium; *TV*, tricuspid valve; *AoP septum*, aorticopulmonary septum; *CT*, conotruncus; *CTS*, conotruncal septum; *SAVC*, superior atrioventricular cushion; *IAVC*, inferior atrioventricular cushion; *AVSD*, atrioventricular cushion defect; and *AoPW*, aorticopulmonary window.

Cardiac anomalies in heterozygous RXRα embryos. We hypothesized that subtle defects in the heterozygous-deficient background may also exist and therefore proceeded to characterize 60 heterozygous embryos; the results are listed in Table I with examples shown in Figs. 5 and 6. Abnormalities at each developmental age are seen in all cardiac tissue types, although less frequent and generally less severe than homozygous embryos. Defects in aortic sac septation are extremely rare as only a single case of pulmonary artery stenosis (2%, Fig. 5 *d*) was observed. Moreover, this likely arose as a secondary, hemodynamically mediated phenomenon subsequent to abnormal conotruncus septation. In this particular embryo, the parietal
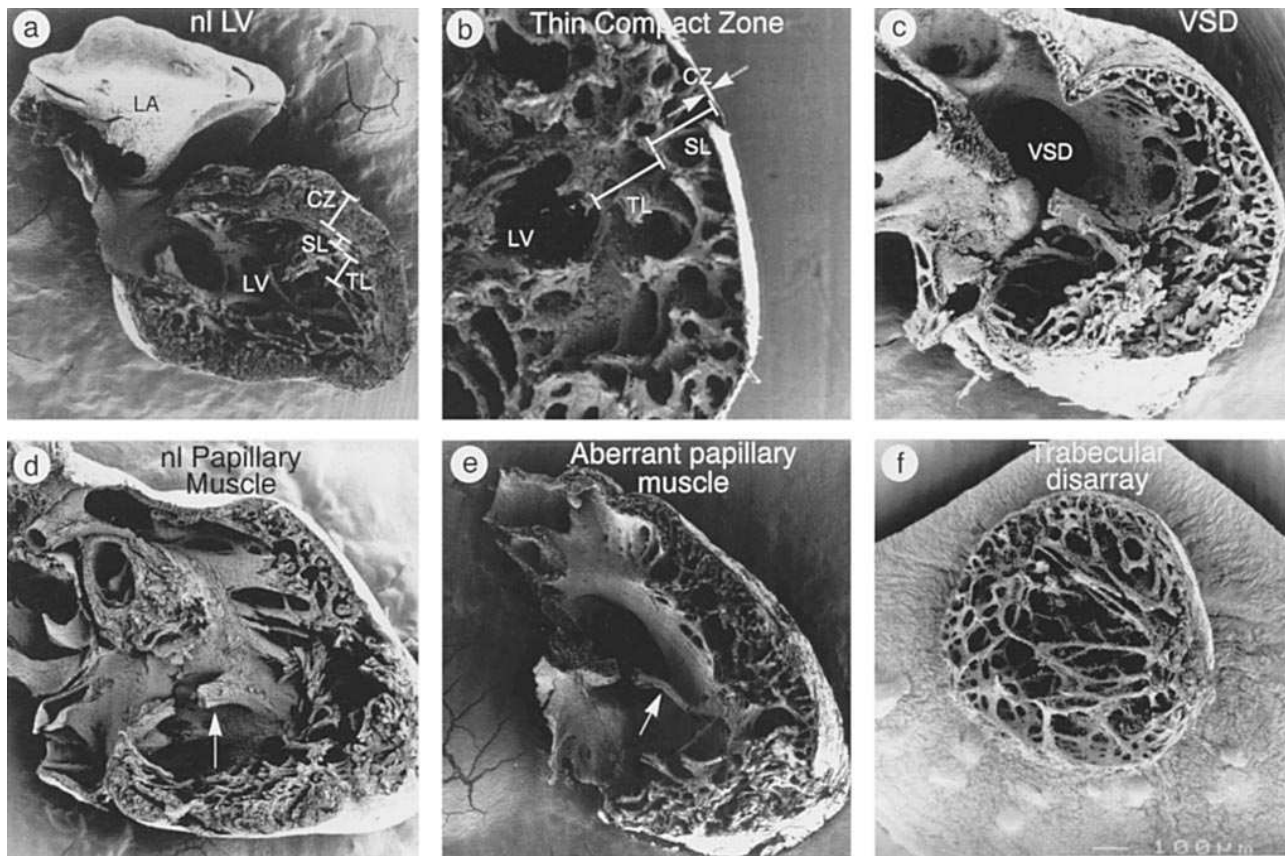
Figure 4. Cardiac muscle defects in *RXRα* −/− embryos. SEM of perfusion-fixed, microdissected *RXRα* −/− mouse embryos demonstrating thin compact zone with expanded spongy layer (*b*), VSD (*c*), aberrant hypoplastic papillary muscle (*arrow*)(*e*), and trabecular disarray (*f*). The first column shows examples of a normal left ventricular chamber (*a*) and papillary muscle (*arrow*, *d*). *LA*, left atrium; *LV*, left ventricle; *VSD*, ventricular septal defect; *CZ*, compact zone; *SL*, spongy layer; *TL*, trabecular layer.

conotruncal ridge was hyperplastic, thereby leading to right ventricular outflow tract obstruction with the resulting reduction in flow likely responsible for the stenotic pulmonary artery. Conotruncal defects were observed in 15% of heterozygous-deficient embryos, with severity ranging from absent conotruncal ridges (3%, Fig. 5 *e*) to a shortened conotruncal septum (7%) with VSD-type DORV (5%). Deficiencies of the atrioventricular cushions were more frequent than those in the conotruncus and ranged from absent fusion (3%) and hypoplasia (8%) to abnormalities of mature valvular structures, such as cleft mitral valve (17%, Fig. 5 *f*), mitral valve stenosis (2%, Fig. 6 *b*), and tricuspid valve abnormalities (8%).

The myocardium was again the most widely affected tissue type resulting in both trabecular (49%) and papillary muscle defects (86%). Close examination of right and left ventricular compact zone (Table II) surprisingly demonstrated an intermediate thickness especially prominent at ed 13.5 and 14.5. In the case of left ventricular wall thickness, there is a significant relationship ($P < 0.03$) between wall thickness and the presence of a cardiac malformation. Severe thinning of the ventricular wall, dubbed "papyraceous phenotype," was seen in both the left (2%, Fig. 6 *b*) and right (2%, Fig. 6 *c*) ventricles, but never simultaneously. Papyraceous left ventricle was associated with mitral valve stenosis yet a perfectly normal right ventricle and semilunar valves. Similarly, papyraceous right ventricle was associated with a dysmorphic tricuspid valve yet

normal left-sided and semilunar structures. In general, trabecular arrangement was less organized in heterozygous embryos than in wild-type embryos.

Intermediate expression level of structural protein MLC-2a. The establishment of anatomical intermediate phenotypes

Table II. Ventricular Wall Thickness in *RXRα* Gene-targeted Embryos

| Ventricle	Stage	Genotype*		
		−/− (18)	+/− (60)	+/+ (29)
Right[‡]	13.5	27.0±4.2	34.6±13.5	67.8±32.9
	14.5	28.3±8.3	42.6±9.8	63.2±5.5
	15.5	22.8±5.6	56.1±10.1	64.3±17.9
Left[§]	13.5	16.7	38.2±5.0	79.2±15.7
	14.5	30.7±15.2	39.7±6.3	69.1±13.2
	15.5	14.2	56.4±24.1	67.3±10.7

*Measurements are in micrometers with a precision of 0.24 μm and presented as mean±SD. [‡]Dependence of right ventricular wall thickness to genotype, $P < 0.0001$. [§]Dependence of left ventricular wall thickness to genotype, $P < 0.0001$.
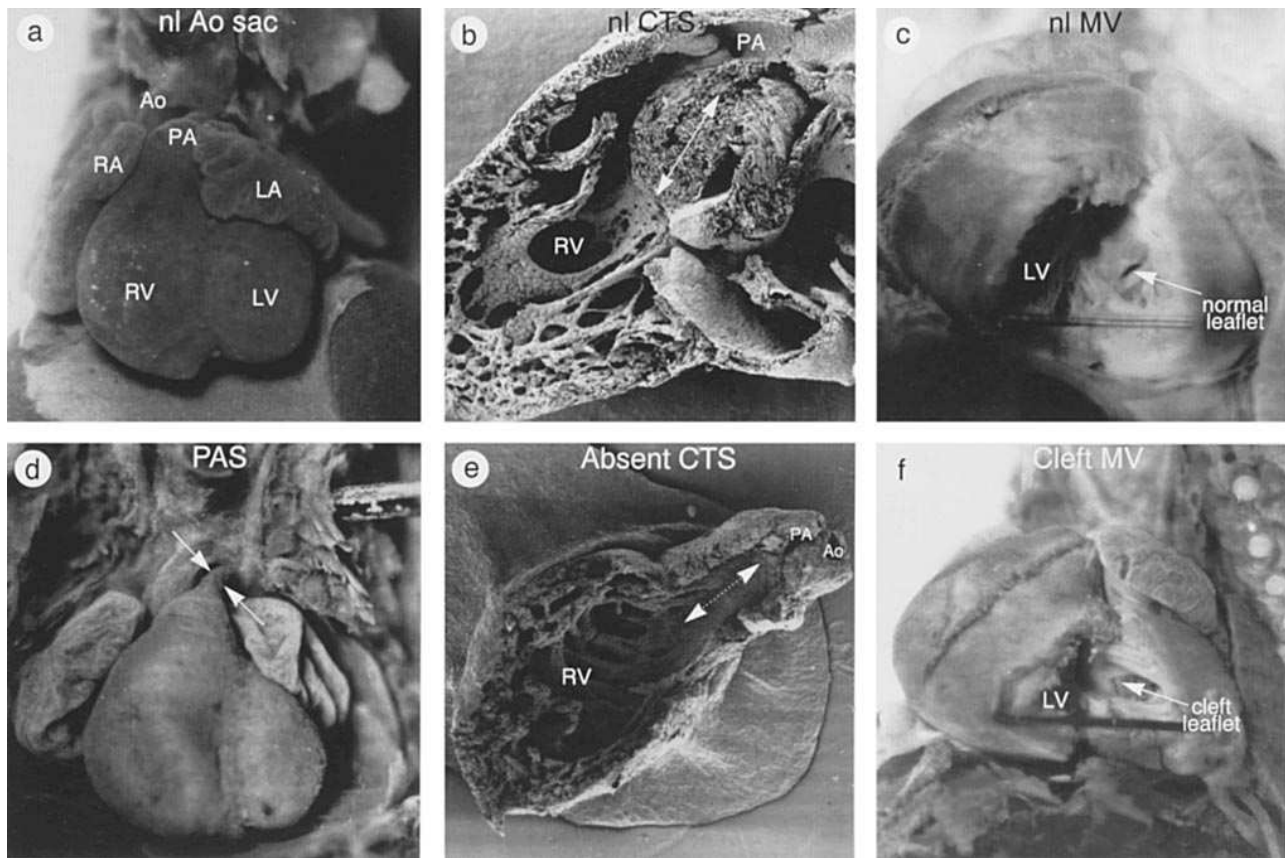
Figure 5. Cushion tissue mesenchyme defects in *RXRα* +/− embryos. Light microphotograph (*a*, *c*, *d*, and *f*) and SEM (*b*, *e*) of perfusion-fixed, microdissected *RXRα* +/− mouse embryos demonstrating aortic sac defects (pulmonary artery stenosis with narrowing indicated by arrows [*d*]), conotruncal defects (hypoplastic conotruncal ridges with double-headed arrows indicating the conotruncal septum [*e*]), and atrioventricular cushion defects (cleft mitral valve [*f*]). The first row shows examples of normal aortic sac (*a*), conotruncus (*b*), and atrioventricular cushion (*c*). *Ao*, aorta; *PA*, pulmonary artery; *RV* right ventricle; *RA*, right atrium; *LV* left ventricle; *LA*, left atrium; *CTR*, conotruncal ridge; *CTS* conotruncal septum; *MV* mitral valve; *PAS*, pulmonary artery stenosis.

in heterozygous embryos implies the existence of molecular correlates. Normally the expression of the structural gene *MLC-2a* follows a pattern in which the gene is expressed throughout the heart until ed 11.0, at which point it is specifi-cally down regulated in the ventricle. However, in *RXRα* −/− embryos, expression of this gene is dysregulated in that expres-sion is maintained to a high level in the ventricle after ed 11.0. Since the ventricles of heterozygous embryos display an inter-
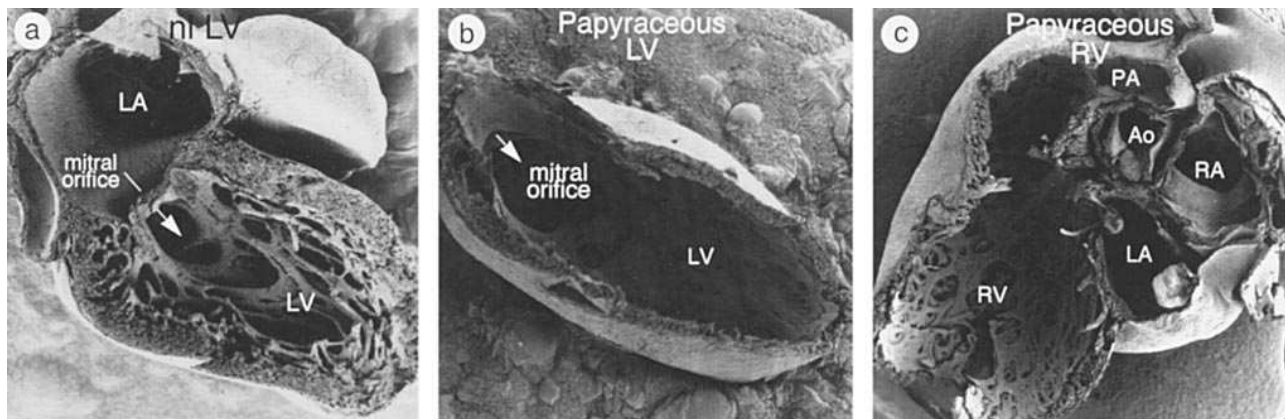
Figure 6. Cardiac muscle defects in *RXRα* +/− embryos. Scanning electron microphotographs of perfusion-fixed, microdissected *RXRα* +/− mouse embryos demonstrating relatively thinned compact zone (*b* and *c*) with papyraceous left *b* and right *c* ventricular walls, trabecular disar-ray (*b* and *c*), and absent papillary muscles (*b* and *c*). The first frame (*a*) shows an example of a normal left ventricular chamber. *Ao*, aorta; *PA*, pulmonary artery; *RV*, right ventricle; *RA*, right atrium; *LV*, left ventricle; *LA*, left atrium.
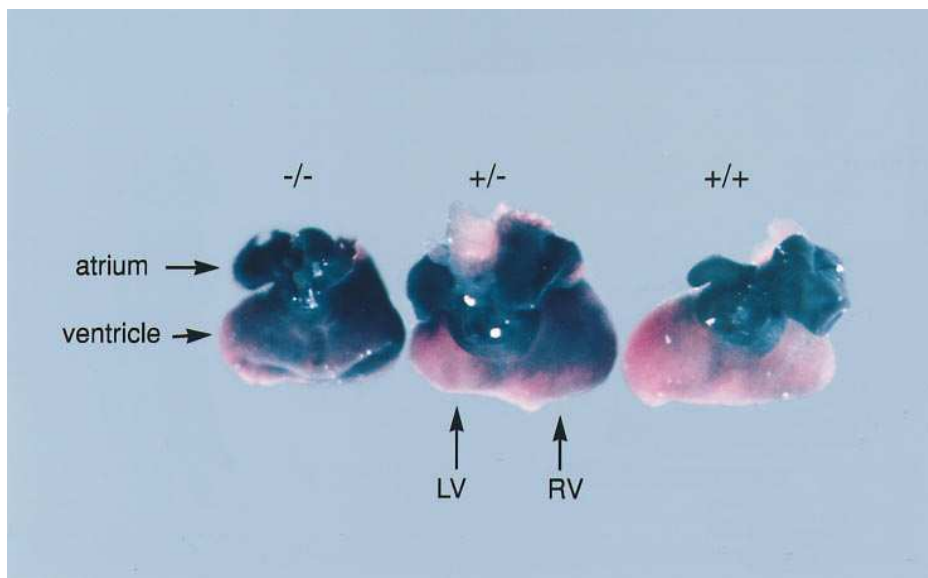
Figure 7. Whole heart (posterior view) MLC-2a in situ hybridization of ed 12.5 *RXRα* gene-targeted mice. Whole heart analysis was performed with a MLC-2a cRNA riboprobe on hearts harvested from a single litter of a *RXRα+/−* to *RXRα+/−* cross. In wild-type animals (*right*), *MLC-2a* transcript is restricted to the atrium, while the ventricle does not stain. In homozygous mutant embryos (*left*), the *MLC-2a* transcript is inappropriately expressed in the ventricle especially in the left ventricle. Heterozygous animals display an intermediate level of expression of *MLC-2a* (*center*).

mediate thickness of the compact zone, we asked the question if the intermediate anatomical phenotypes were reflected in an intermediate level of *MLC-2a*.

To precisely delineate the normal expression pattern of *MLC-2a*, we used whole mount in situ procedures. Usually, these are difficult to perform for embryos older than ed 10.0; however, by the introduction of small modifications in the procedure and the combination of microdissection, we were able to perform whole heart in situ with good fidelity up to ed 14.0. Fig. 7 demonstrates *MLC-2a* whole heart expression patterns from embryos from wild-type, heterozygous, and homozygous *RXRα* embryos. Homozygous embryos show increased expression of *MLC-2a* throughout the ventricles, both right and left, compared to wild-type embryos. Interestingly, heterozygous embryos display an intermediate expression level. This reflects the intermediate anatomic phenotypic severity seen in both ventricular wall thickness and atrioventricular valvular morphology. In addition, among heterozygous embryos, expression of *MLC-2a* is variable, though always higher than wild-type embryos and lower than homozygous embryos. This again reflects the anatomic analysis in which there exists large phenotypic variability.

Although whole heart in situ appears to be a valid technique for spatial localization of transcripts in post–ed 10.0 hearts, it is poorly quantitative. To fully characterize *MLC-2a* expression levels, we performed RNase protection assays on left ventricular free wall samples to examine quantitative *MLC-2a* gene expression in each genotype. Protection assays were performed on single heart tissue samples in order to reduce variability that may be introduced at various steps of RNA isolation or processing. Embryonic hearts from littermates were dissected free from constitutive *MLC-2a*–expressing cardiac tissues; i.e., ventricular outflow tracts and atria. RNase protection assays were simultaneously performed on these samples using riboprobes for *MLC-2a* and the internal control, *EF-1α*. The results of these experiments are shown in Fig. 8. As seen in both the anatomical analysis and the molecular spatial analysis, heterozygous embryos display an intermediate level of *MLC-2a* expression between wild-type and homozygous embryos. Lane *1* shows a wild-type embryo, lanes *2–7*

heterozygotes, and lane *8*, a homozygote. Riboprobes protect transcripts from the *MLC-2a* gene (*upper band*) and structural protein EF-1α gene (*lower band*). *EF-1α* expression level was independent of genotype and unchanged, while *MLC-2a* expression levels segregated with genotype. Homozygous embryos demonstrated a more than twofold increase in normalized expression level over homozygous embryos, while heterozygous embryos had an intermediate expression level in agreement with the whole heart in situ data. Due to the morphologically destructive nature of both the microdissection/SEM and RNase protection assays, we were unable to correlate *MLC-2a* expression levels with severity of anatomic phenotype.

Therefore, we have shown that the structural gene *MLC-2a* is a quantitative molecular marker for the heterozygous phe-

	+/+	+/-					-/-
Norm 2a	1.41	1.78	1.89	2.16	1.77	1.93	3.21
Fold +/+	1.00	1.26	1.34	1.53	1.26	1.37	2.28
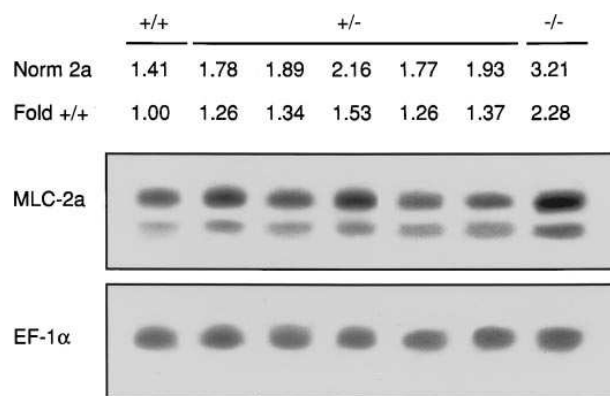
Figure 8. RNase protection assay of ed 13.5 *RXRα* gene-targeted mice. RNase protection assays were performed on isolated hearts from ed 13.5 murine embryos. The figure represents hearts from all members of a single litter of a *RXRα+/−* to *RXRα+/−* cross. Simultaneous hybridization of RNA extracts was performed with cRNA probes for *MLC-2a* (*upper band*) and EF-1α (*lower band*). Expression of the atrial marker *MLC-2a* was increased in the homozygous embryo (*right*) with respect to the wild-type control (*left*). Heterozygous embryos displayed a variable, intermediate level of *MLC-2a* expression always higher than wild-type and lower than homozygous embryos.
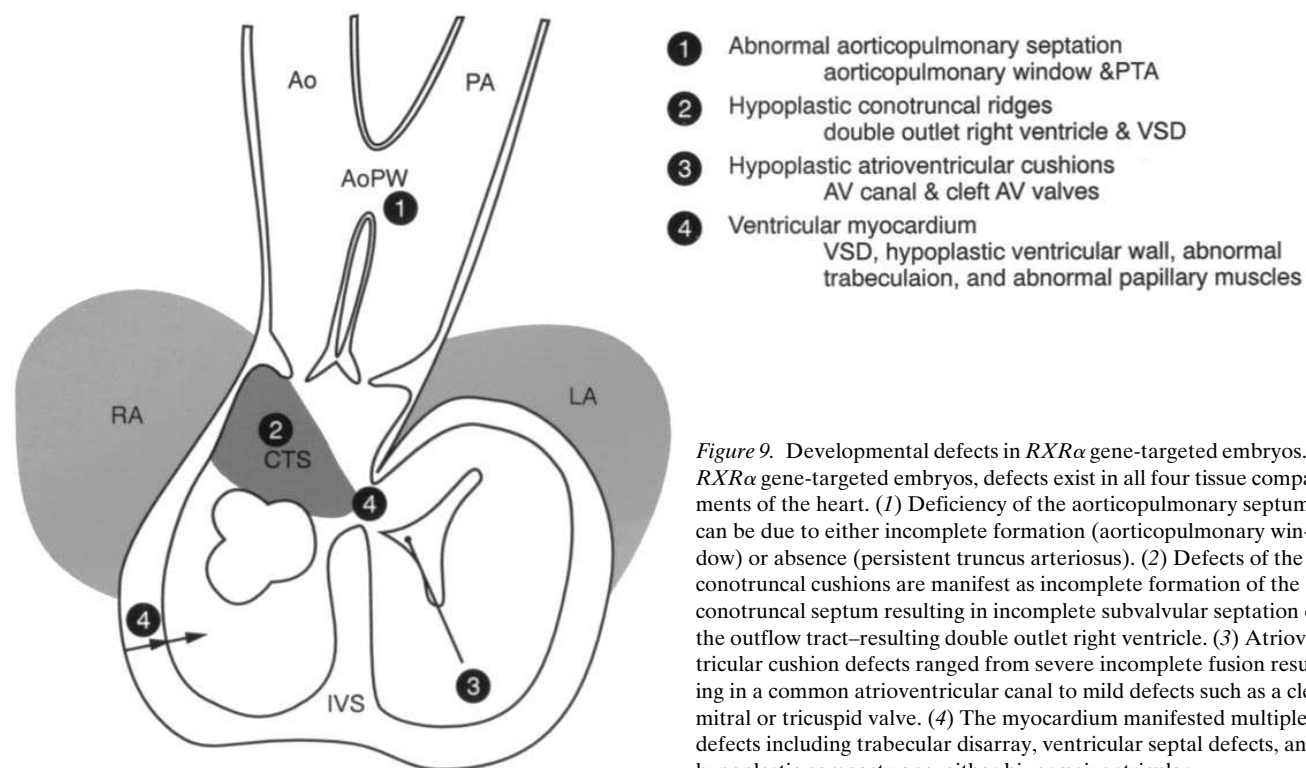
notype with an intermediate expression level between wild-type and homozygous embryos. In addition, these findings further strengthen the hypothesis that *RXRα* gene dosage plays an important role in determining the structural phenotype of the developing heart.

Discussion

RXRα deficiency produces multiple defects in the aortic sac, conotruncal ridges and atrioventricular cushions, and ventricular chamber. By analyzing a large number (107) of the wild-type and *RXRα* gene–targeted embryos with a combination of systematic microdissection and SEM to diagnose and quantitatively score all the potential morphogenic defects in each cardiac compartment, we have uncovered a large array of cardiac abnormalities in *RXRα*-deficient murine embryos (Fig. 9). Within the ventricular chambers, SEM provides clear evidence, not only of the previously described defect in expansion of the compact zone, but also of defects in trabecular morphogenesis achieving neither the appropriate orientation nor thickness to form mature trabeculae. These studies imply that *RXRα* may play an important role not only in expansion of the compact zone, but also in controlling the entire process of trabecular morphogenesis, which is likely to be a critical step in chamber development. Accompanying these ventricular muscle abnormalities were widespread defects in other tissue compartments within the heart. In the outflow tract, neural crest migration and cushion tissue mesenchyme formation are both required for normal septation, resulting in the formation of the aortic and pulmonary outflow tracts. Some *RXRα* homozygous-deficient embryos demonstrated PTA (11%) with largely deficient aorticopulmonary septation, yet in the absence of any other signs indicative of a more generalized neural crest defi-

ciency (i.e., aortic arch abnormalities). More frequently (28%), an aorticopulmonary window was found that results in a partial communication between the great vessels above the level of the semilunar valves. The mechanism responsible for the aorticopulmonary septum defects is unclear, but is unlikely to be due to widespread defects in neural crest formation or migration, which are not seen in the RXRα −/− background. Thus, these studies suggest a specific requirement for RXRα in the formation of aortic sac mesenchyme. However, the possibility exists that the neighboring ventricular muscle cells that lie in the subvalvular region might also somehow be important for sending appropriate cues for the septation of the proximal region of the aortic sac. One of the major questions will be to determine whether there are separate requirements for RXRα in the formation of cardiac mesenchyme and muscle, and the potential relationships between these important events during heart morphogenesis. One could explore the presumptive cell autonomous nature of the myocardial defect by transplanting mutant cells into wild-type embryos and looking for rescue of the cellular phenotype; these studies are currently underway. This primary myocardial cell hypothesis is further strengthened by the observation that defects in the outflow tract are rare, and these tissues are not known to be influenced by the myocardium.

A similar requirement for *RXRα* in the formation of conotruncal ridges and atrioventricular cushion was also observed. DORV, which in the VSD form occurs due to hypoplasia of the conotruncal ridges, represented a phenocopy of the specific pathology seen in man. Atrioventricular endocardial cushion defects were also observed due to lack of fusion of the superior and inferior endocardial cushions. Taken together, the range of defects seen in the aorticopulmonary septum, conotruncal ridges, and atrioventricular cushions indicate that

1. Abnormal aorticopulmonary septation
   aorticopulmonary window &PTA
2. Hypoplastic conotruncal ridges
   double outlet right ventricle & VSD
3. Hypoplastic atrioventricular cushions
   AV canal & cleft AV valves
4. Ventricular myocardium
   VSD, hypoplastic ventricular wall, abnormal trabeculaion, and abnormal papillary muscles

Figure 9. Developmental defects in *RXRα* gene-targeted embryos. In *RXRα* gene-targeted embryos, defects exist in all four tissue compartments of the heart. (*1*) Deficiency of the aorticopulmonary septum can be due to either incomplete formation (aorticopulmonary window) or absence (persistent truncus arteriosus). (*2*) Defects of the conotruncal cushions are manifest as incomplete formation of the conotruncal septum resulting in incomplete subvalvular septation of the outflow tract–resulting double outlet right ventricle. (*3*) Atrioventricular cushion defects ranged from severe incomplete fusion resulting in a common atrioventricular canal to mild defects such as a cleft mitral or tricuspid valve. (*4*) The myocardium manifested multiple defects including trabecular disarray, ventricular septal defects, and hypoplastic compact zone, either bi- or univentricular.

there may be an *RXRα* requirement not only for ventricular chamber expansion in the compact zone and appropriate myocardial architecture development, but also for the morphogenesis of nonmuscle compartments.

The question arises as to whether these various defects in each of the cardiac segments (aortic sac, conotruncus, atrioventricular cushion, and ventricular chamber) represent single or distinct requirements for *RXRα*-dependent pathways. The ventricular chamber defect is associated with maturational arrest of ventricular muscle cells within the *RXRα* −/− embryos that is manifest by the persistent expression of an atrial marker (MLC-2a) (18). The timing of this block in ventricular maturation places a requirement for *RXRα* between ed 10.0- and 12.0, just around the time of the decrease in cardiac chamber function in these embryos (18). Interestingly, this is just after initiation of aortic sac and atrioventricular canal septation. The latter structure results from an epithelial-to-mesenchymal transformation based upon initial cues from the overlying myocardium. In both mouse and man, the conotruncal ridges are two structures that arise in the proximal portion of the outflow tract. This subvalvular septation of the outflow tract is responsible for directing the flow of blood from the left ventricle to the aorta and the right ventricle to the pulmonary artery and is due to fusion of the conotruncal ridges. Lack of fusion of the conotruncal ridges results in incomplete formation of the conotruncal septum resulting in DORV. The atrioventricular cushions bear a phenotype similar to those of the conotruncus. Again, in the majority of cases, formation of primordial cushion tissue is initiated; however, the further development of this tissue appears defective in the *RXRα* −/− embryos. Since the initial molecular cues for cushion formation are derived from neighboring cardiac muscle cells, the possibility exists that the cushion defects arise, in part, due to a primary defect in the cardiac muscle cell. If such is the case, the defects in the cushion tissue mesenchyme might arise as a result of a requirement for *RXRα*, not in the endocardial or mesenchymal cells per se, but in the neighboring muscle cells that fail to elicit an appropriate signal. Alternatively, the defect may be secondary to incomplete fusion of the cushions.

RXRα heterozygous deficiency confers genetic susceptibility for cardiac morphogenic defects. To date, evidence for cardiac defects in mice that are heterozygous deficient for an individual member of the retinoid gene family have not been described. To our knowledge, the *RXRα* −/− mice embryos are the only single gene–targeted embryos within the retinoid receptor gene family that display cardiac defects. Although combined double and triple knockouts of other receptors result in cardiac defects, these defects have not occurred in embryos harboring deficiencies in only a single member of the retinoid receptor gene family (11–17). As such, *RXRα* appears to play a particularly important role in cardiac morphogenesis. This result was underscored by the findings in the current study, which surprisingly uncovered an intermediate phenotype in heterozygous embryos. While these embryos display normal ventricular function at ed 14.5, they nevertheless provide evidence of an intermediate phenotype in the ventricular chamber morphology, manifested by a compact zone of intermediate thickness, and aberrant trabecular architecture. In fact, in some embryos, complete absence of the papillary muscles was noted. Selective hypoplasia of either the left or right ventricular chamber was also evident.

In addition to defects in ventricular muscle, there was also clear-cut evidence of atrioventricular cushion defects that ranged from complete atrioventricular canal to cleft mitral valve, an indication of abnormal or incomplete fusion of the superior and inferior atrioventricular cushions. The ventricular chamber displayed the most sensitivity to *RXRα* deficiency, as the majority of heterozygous-deficient embryos displayed a defect. However, malformations of the atrioventricular cushion, conotruncal region, and in the aortic sac were variable, implying that relative *RXRα* deficiency confers genetic susceptibility for these morphogenic defects. These observations in the heterozygous-deficient *RXRα* +/− embryos suggest a threshold effect for *RXRα* actions in these distinct regions of the developing heart, again implying that there may be multiple spatial and temporal requirements for *RXRα* within each one of these cardiac compartments. As such, *RXRα* may play a particularly important role in coordinating several events during the course of cardiac morphogenesis. Alternatively, a relative deficiency in *RXRα* might increase the propensity for these cardiac malformations through retinoid-dependent pathways. This particular scenario is analogous to the proposed role of p53 in which deficiency confers susceptibility to multiple, distinct oncologic phenotypes while determining specificity for none (23). Similarly, *RXRα* confers genetic susceptibility for multiple congenital heart disease phenotypes by disturbing normal development in four distinct structures of the heart, aorticopulmonary septum, conotruncal ridges, atrioventricular cushions, and ventricular myocardium.

RXRα deficiency produces phenocopies of congenital heart disease in man. Since complete *RXRα* deficiency in the homozygous embryos is associated with midgestation embryonic lethality, it is unlikely that this homozygous-deficient genotype accounts for a substantial fraction of surviving congenital heart disease. However, finding that the heterozygous-deficient *RXRα* +/− embryos can display an array of congenital heart phenotypes suggests the possibility that *RXRα*, components of its downstream signaling pathway, or their targets may play an important role in the etiology of congenital heart disease in man. On one hand, they may play a role in conferring genetic susceptibility through genes that either modify the phenotype or are responsible for the particular congenital heart disease phenotype. Alternatively, the defects might arise primarily through a complete or relative deficiency in *RXRα*. Since *RXRα* exerts its effects primarily through the regulation of downstream target genes, the possibility exists that the target genes themselves may play a particularly important role in producing these congenital heart disease phenotypes. In this regard, we have already isolated a number of candidate genes by subtraction cloning that are inappropriately expressed in *RXRα* −/− embryos, and are in the process of identifying whether these are indeed aberrantly expressed in the region of embryos that display specific cardiac anomalies. It will be interesting to directly examine this possibility in cases of congenital heart disease in man that are not ascribed to other genetic backgrounds, such as Down's syndrome, CATCH-22, or Holt-Oram syndrome. Since sporadic cases account for a large number of congenital heart disease cases, the possibility also exists that *RXRα* or components of its downstream signaling pathway may play a role in these instances. The availability of this model system should be instrumental in allowing the eventual identification of components of the *RXRα* signaling pathway that may play important roles in the onset of these specific cardiac malformations (Ruiz-Lozano, P., S.W. Kubalak, H.M. Su-

cov, R.M. Evans, and K.R. Chien, unpublished results). Understanding the potential role of genetic background possibly in combination with maternal nutrient status in the production of these various defects can also be explained in the mouse model system. This study also underscores the utility of using appropriate approaches to score for the frequency, severity, and complexity of congenital heart disease phenotypes in an efficient fashion, and should prove useful in analyzing other gene-targeted embryos that harbor cardiovascular anomalies.

Acknowledgments

References

1. Payne, R.M., M.C. Johnson, J.W. Grant, and A.W. Strauss. 1995. Toward a molecular understanding of congenital heart disease. *Circulation.* 91:494–504.

2. Curran, M.E., D.L. Atkinson, A.K. Ewart, C.A. Morris, M.F. Leppert, and M.T. Keating. 1993. The elastin gene is disrupted by a translocation associated with supravalvular aortic stenosis. *Cell.* 73:159–168.

3. Basson, C.T., G.S. Cowley, S.D. Solomon, B. Weissman, A.K. Poznanski, T.A. Traill, J.G. Seidman, and C.E. Seidman. 1993. The clinical and genetic spectrum of the Holt-Oram syndrome (Hand-Heart syndrome). *N. Engl. J. Med.* 330:885–891.

4. Budarf, M.L., J. Collins, W. Gong, B. Roe, Z. Wang, L.C. Bailey, B. Sellinger, D. Michaud, D.A. Driscoll, and B.S. Emanuel. 1995. Cloning a balanced translocation associated with DiGeorge syndrome and identification of a disrupted candidate gene. *Nat. Genet.* 10:269–277.

5. Burn, J., A. Takao, D. Wilson, I. Cross, K. Momma, R. Wadey, P. Scambler, and J. Goodship. 1993. Conotruncal anomaly face syndrome is associated with a deletion within chromosome 22q11. *J. Med. Genet.* 30:807–812.

6. de la Chapelle, A., R. Herva, M. Koivista, and P. Aula. 1981. A deletion in chromosome 22 can cause DiGeorge syndrome. *Hum. Genet.* 57:253–256.

7. Goldmuntz, E., D. Driscoll, M.L. Budarf, E.H. Zackai, D.M. McDonald-McGinn, J.A. Biegel, and B.S. Emanuel. 1993. Microdeletions of chromosomal region 22q11 in patients with congenital conotruncal cardiac defects. *J. Med.*
Genet. 30:807–812.

8. Lammer, E.J., D.T. Chen, R.M. Hoar, N.D. Agnish, P.J. Benke, J.T. Braun, C.J. Curry, P.M. Fernhoff, A.W. Grix Jr., I.T. Lott, et al. 1985. Retinoic acid embryopathy. *N. Engl. J. Med.* 313:837–841.

9. Wilson, J.G., and J. Warkany. 1949. Aortic-arch and cardiac anomalies in offspring of vitamin A deficient rats. *Am. J. Anat.* 83:113–155.

10. Wilson, J.G., C.B. Roth, and J. Warkany. 1953. An analysis of the syndrome of malformations induced by maternal vitamin A deficiency. Effects of restoration of vitamin A at various times during gestation. *Am. J. Anat.* 92:189–217.

11. Li, E., H.M. Sucov, K.F. Lee, R.M. Evans, and R. Jaenisch. 1993. Normal development and growth of mice carrying a targeted disruption of the alpha 1 retinoic acid receptor gene. *Proc. Natl. Acad. Sci. USA.* 90:1590–1594.

12. Lufkin, T., D. Lohnes, M. Mark, A. Dierich, P. Gorry, M.P. Gaub, M. LeMeur, and P. Chambon. 1993. High postnatal letahlity and testis degeneration in retinoic acid receptor alpha mutant mice. *Proc. Natl. Acad. Sci. USA.* 90:7225–7229.

13. Mendelsohn, C., M. Mark, P. Dolle, A. Dierich, M.P. Gaub, A. Krust, C. Lampron, and P. Chambon. 1994. Retinoic acid receptor beta 2 (RAR beta 2) null mutant mice appear normal. *Dev. Biol.* 166:246–258.

14. Lohnes, D., P. Kastner, A. Dierich, M. Mark, M. LeMeur, and P. Chambon. 1993. Function of retinoic acid receptor gamma in the mouse. *Cell.* 73:643–658.

15. Mendelsohn, C., D. Lohnes, D. Decimo, T. Lufkin, M. LeMeur, P. Chambon, and M. Mark. 1994. Function of the retinoic acid receptors (RARs) during develoment (II). Multiple abnormalities at various states of organogenesis in RAR double mutants. *Development (Camb.).* 120:2749–2771.

16. Sucov, H.M., E. Dyson, C.L. Gumeringer, J. Price, K.R. Chien, and R.M. Evans. 1994. RXRα mutant mice establish a genetic basis for vitamin A signaling in heart morphogenesis. *Genes Dev.* 8:1007–1018.

17. Kastner, P., J.M. Grondona, M. Mark, A. Gansmuller, M. LeMeur, D. Decimo, J.L. Vonesch, P. Dolle, and P. Chambon. 1994. Genetic analysis of RXRα developmental function: convergence of RXR and RAR signaling pathways in heart and eye morphogenesis. *Cell.* 78:987–1003.

18. Dyson, E., H.M. Sukov, S.W. Kubalak, G. Schmid Schönbein, F. Delano, R.M. Evans, J. Ross, and K.R. Chien. 1995. Atrial-like phenotype is associated with embryonic ventricular failure in RXRα -/- mice. *Proc. Natl. Acad. Sci. USA.* 92:7386–7390.

19. Pexieder, T. 1986. Standardized method for study of normal and abnormal cardiac development in chick, rat, mouse, dog, and human embryos. *Teratology.* 33:91C–92C.

20. Pexieder, T. 1981. Prenatal development of the endocardium: a review. *Scanning Electron Microscopy* 2:223–253.

21. Moscoso, G., and T. Pexieder. 1990. Variations in microscopic anatomy and ultrastructure of human embryonic hearts subjected to three different modes of fixation. *Pathol. Res. Pract.* 186:768–774.

22. Wilkinson, D.G. 1992. Whole mount in situ hybridization of vertebrate embryos. *In In situ* Hybridization: A Practical Approach. IRL Press, Oxford, UK. 155–171.

23. Harvey, M., H. Vogel, D. Morris, A. Bradley, A. Bernstein, and L.A. Donehower. 1995. A mutant p53 transgene accelerates tumor development in heterozygous but not nullizygous p53-deficient mice. *Nat. Genet.* 9:305–311.